11th Australasian Fluid Mechanics Conference
University of Tasmania, Hobart, Australia
14-18 December 1992

VISUALISATION OF A CIRCULAR CYLINDER NEAR-WAKE FLOW FIELD BY A CAFV TECHNIQUE

Ryoji WAKA[1], Fumio YOSHINO[1], Tsutomo HAYASHI[1] and Seiji TAKEBAYASHI[2]

[1]Dept of Mechanical Engineering, Tottori University, Koyama, Tottori 680, JAPAN

[2]TOYOBO Company Ltd, Iwakuni, Yamaguchi, JAPAN

ABSTRACT

The velocity vectors were determined with a hot-wire probe of three-wires type in a near-wake flow field of a circular cylinder except the region just behind the cylinder. The *general* hot-wire response equations and a phase-averaging technique were applied to measurement of the velocity vectors. The periodically fluctuating velocity vectors associated with shedding of Kármán vortices were also extracted from the phase-averaged velocity vectors. Both of them were visualized as an animation by applying a CAFV technique. Not only the periodic fluctuation of the near-wake flow field but also the Kármán vortices rolling up behind the circular cylinder were clearly visualized.

It was confirmed that the velocity vector fields measured by the present method were considerably consistent with the computational results. The measuring method proposed here may be applied to various flow fields associated with a periodic fluctuation.

INTRODUCTION

A near-wake flow field of a bluff body such as a circular cylinder is one of the most difficult flow fields to measure the velocity vectors. It is because it exhibits a very strong unsteadiness, that is, because both the magnitude and the direction of the velocity vector are periodically and heavily fluctuating with time. Though many investigations on the flow visualization have been carried out by using numerical simulations and the various traditional techniques (Perry et al., 1982) a few of the established measuring methods with a hot-wire anemometer were successfully used to obtain the reliable results of velocity vector fields in the near-wake of the bluff body (Cantwell and Coles, 1983, Tanaka and Murata, 1985).

The objectives of the present study are to attempt to establish the measuring method with a hot-wire probe of three-wires type and to visualize the near-wake flow field of a circular cylinder on the basis of a phase-averaging and a CAFV (Computer Aided Flow Visualization) techniques.

HOT-WIRE RESPONSE EQUATIONS

A response equation of the hot-wire used in this paper represents the relation of an effective cooling velocity (Ue) to the instantaneous velocity components (U,V,W) on the coordinate system (X,Y,Z) fixed in the flow field (refer to Fig.2). Yoshino et al. (1989) described a derivation of a *general* response equation of the hot-wire set arbitrarily in a flow field in detail and it was given in Eq.(5) in that reference (Yoshino et al., 1989).

Now, all the hot-wires used in the present experiment are set in the vertical plane (X-Y) at the mid-span of the cylinder, which is perpendicular to the central axis (Z) of the cylinder. Assuming that both the main flow and periodically fluctuating velocities are two-dimensional, the instantaneous velocity components are expressed as follows;

$$U = \overline{U} + \tilde{u} + u' \tag{1}$$

$$V = \overline{V} + \tilde{v} + v' \tag{2}$$

$$W = w' \tag{3}$$

where $(\overline{U},\overline{V})$, $(\tilde{u},\tilde{v})$ and (u',v',w') are the time mean, the periodically fluctuating and the turbulence velocity components in the coordinate system (X,Y,Z), respectively.

Then the hot-wire response equations of I-type and X-type probes are derived from the *general* response equation as following equations;

$$U_{eI}^2 = \{\cos^2\gamma + k^2\sin^2\gamma\}U^2 + \{\sin^2\gamma + k^2\cos^2\gamma\}V^2 + h^2W^2 + (1-k^2)\cdot UV \tag{4}$$

$$U_{e+}^2 = \frac{1}{2}\{(1+k^2) + (1-k^2)\sin 2\gamma\}U^2 + \frac{1}{2}\{(1+k^2) - (1-k^2)\sin 2\gamma\}V^2 + h^2W^2 - (1-k^2)\cos 2\gamma \cdot UV \tag{5}$$

$$U_{e-}^2 = \frac{1}{2}\{(1+k^2) - (1-k^2)\sin 2\gamma\}U^2 + \frac{1}{2}\{(1+k^2) + (1-k^2)\sin 2\gamma\}V^2 + h^2W^2 + (1-k^2)\cos 2\gamma \cdot UV \tag{6}$$

where U_{eI}, U_{e+} and U_{e-} are effective cooling velocities for I-type and X-type probes, respectively and γ is the rotational angle around the Z axis. Also k (=0.1) and h (=1.1) are yaw and pitch factors, respectively, and they are assumed as constant in the present study.

Elimination of the term of W^2 and substitution of Eq.(4) into Eq.(5) and Eq.(6) yield the relations of effective cooling velocities of all the hot-wires to the velocity components (U,V) in X-Y plane as follows;

$$U^2 - V^2 = \frac{(U_{e+}^2 - U_{e-}^2)\sin 2\gamma - (U_{e+}^2 + U_{e-}^2 - 2U_{eI}^2)\cos 2\gamma}{1-k^2} \tag{7}$$

$$UV = \frac{-(U_{e+}^2 - U_{e-}^2)\cos 2\gamma - (U_{e+}^2 + U_{e-}^2 - 2U_{el}^2)\sin 2\gamma}{2(1-k^2)} \quad (8)$$

Now solving the above equations as simultaneous equations, the instantaneous velocity components, U and V, are obtained as a function of the effective cooling velocities. In the present experiment, a constant temperature hot-wire anemometer with a lineariser was used for each hot-wire, so that the output voltage (E) from the hot-wire anemometer was proportional to the effective cooling velocity (U_e). Then the relation of E to U_e is expressed in Eq.(9) for each hot-wire.

$$E = SU_e \quad (9)$$

where S is a sensitivity of the hot-wire.

PHASES ON A REFERENCE SIGNAL

The reference signal for phase-averaging was obtained as a sinusoidal curve shown in figure 1. This figure shows the time history of the reference signal and the reference phases for phase-averaging were determined in the following procedures. First, four (4) fundamental phases were selected on the reference signal. Each of the four (4) phases was selected in such a way that the output voltage (E) of the reference signal and its derivative satisfied one of the following conditions concerning the output voltage and its time derivative (dE/dt), that is, (E=0, dE/dt>0), (E>0, dE/dt=0), (E=0, dE/dt<0) and (E<0,dE/dt=0) shown in figure 1. Next, thirty-two (32) phases were determined on the reference signal by further dividing the time intervals between two consecutive fundamental phases into equal eight (8) parts. These phases are named Phase 1 to Phase 32 and expressed as 1/32 to 32/32 in figure 1.

EXPERIMENTAL APPARATUS AND METHOD

Fig.2 shows the test-section of the wind tunnel. The circular cylinder model with a diameter(D) of 100mm is mounted at the center of the test-section and passes through two partition-plates and the side-walls of the tunnel. The outer surface of the cylinder is sufficiently smooth. The value of aspect ratio of the cylinder is adjusted to be eight (8) by moving the partition-plates in the test-section.The solid blockage ratio of the test-section is about 0.14 and the turbulence intensity of the free stream is less than 0.2%.

The experiment was carried out at the constant Reynolds number(Re) of 1.0×10^5, which was based on the cylinder diameter(D) and the free stream velocity(U_∞). Then the shedding frequency of Kármán vortices and the Strouhal number were about 30Hz and 0.19, respectively.

The phase-averaged velocity vectors were determined in the near wake region of the cylinder showed by the oblique lined area in figure 3, except the region just behind the cylinder. The reference signal was detected at the point, (X/D,Y/D)=(1.2,1.7), in the potential flow region outside the wake flow of the cylinder with an I-type hot-wire probe. The measuring time at each point was 10 seconds and it corresponded to about 300 cycles of Kármán vortex shedding from the cylinder.

Fig.4 shows a block diagram of the measuring system. The output signal from the hot-wire (Wire 1) anemometer was amplified by a DC amplifier to get a sinusoidal signal with the amplitude large enough as a reference signal, after passing through the band-pass filter with a passing band of 25Hz to

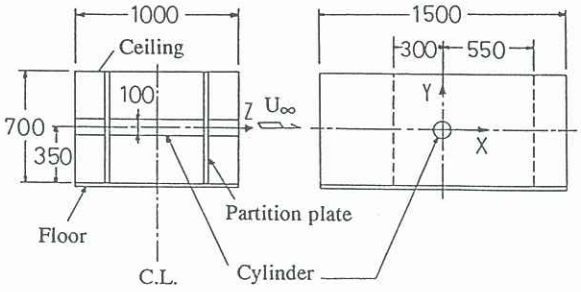

Fig.2 Test-section of wind tunnel

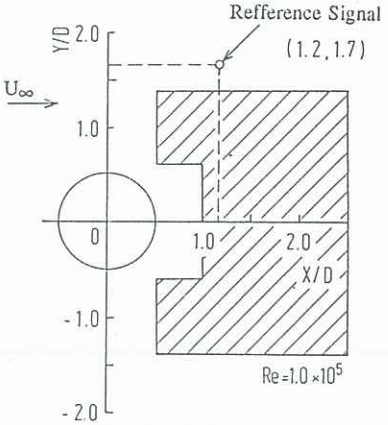

Fig.3 Measuring area

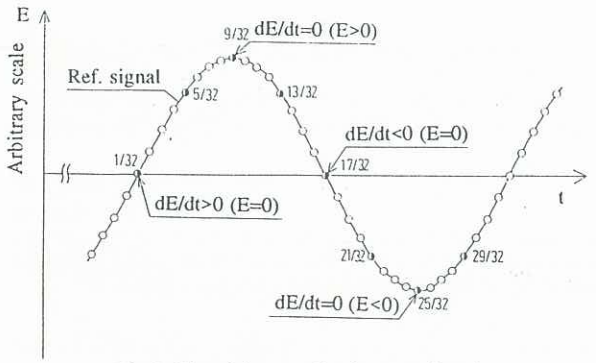

Fig.1 Time history of reference signal

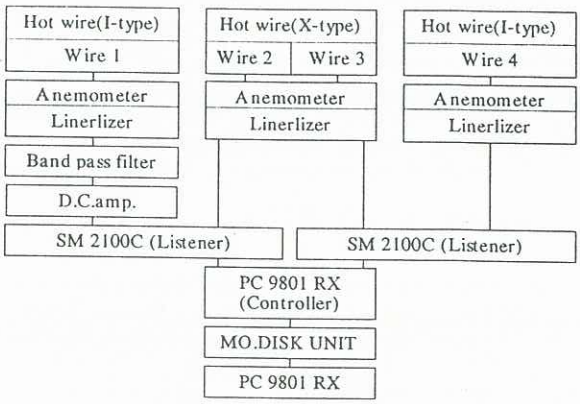

Fig.4 Block diagram of measuring system

35Hz.

EXPERIMENTAL RESULTS AND DISCUSSION

Calibration of the Experimental Method

The experimental method proposed here was calibrated with an I-type hot-wire probe in the core region of a circular free jet for various jet velocities. The exit diameter of the nozzle was 30mm and its contraction ratio was 9/100. The results of the calibration are shown in figure 5. θ_s is rotational angle of the hot-wire probe around the central axis of the circular free jet and θ_m is the angle measured by present method under an arbitrary setting angle of the hot-wire probe (θ_s). It is found from these figures that the measured angle (θ_m) is considerably consistent with the setting angle (θ_s) for all the jet velocities, except for the case that the setting angle of the hot-wire is greater than about +70 degree or less than about -70 degree, and the measuring accuracy of the velocity is also sufficient within the experimental range of velocities.

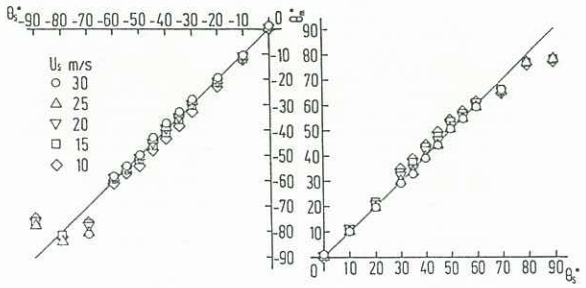

Fig.5 Calibration of experimental method

The experimental results of the phase-averaged and the periodically fluctuating velocity vector fields are compared with the results computed by using a discrete vortex method (Inamuro, 1988) in figure 6(a)~(d). The results of computation shown in these figures were quoted from the results at the nondimensional time T* ($=U_\infty T/D$) of 15.0 and 18.0, where T is an elapsed time from outset of computation. Fig.6(a) and (b) show the streamlines behind the cylinder at T*=15.0 and 18.0, respectively, and Fig.6(c) and (d) show the distributions of discrete vortices shed downstream from the separation points on the cylinder at the same times (T*) with Fig.6(a) and (b), respectively. This comparison will be reasonable, because the near-wake of the cylinder may be able to be regarded as a completely periodic flow field at T*=15.0. And it will be found from figure 7 which shows the time history of the lift coefficient acting on the cylinder represented as a function of T*.

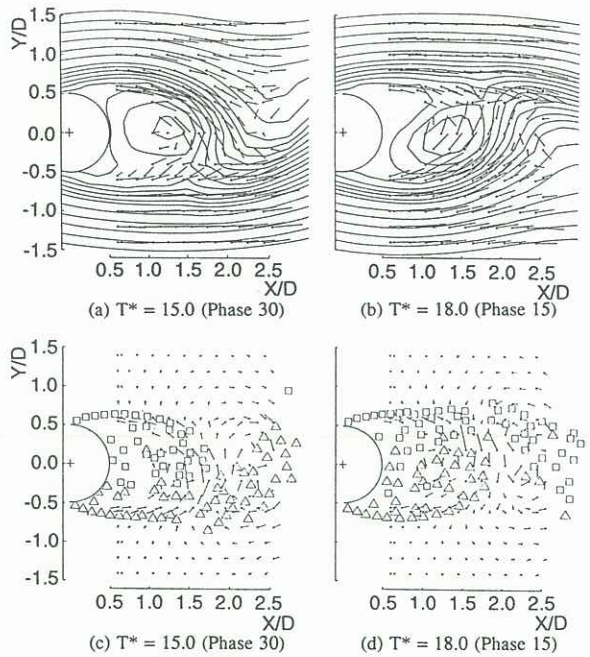

Fig.6 Comparison with computational results

Phase-Averaged Velocity Vector Fields

Fig.8(a)~(h) show the phase-averaged velocity vector fields at the typical eight (8) phases out of thirty-two (32) phases. The mark (●) expresses the measuring point and the segmental length suggests the magnitude of velocity vector.An up-and-down variation of the near-wake flow field is clearly visualized. The flow patterns are shifted each other by half the shedding period of Kármán vortex, for example Phase 1 and Phase 17, and are almost symmetric with respect to X axis. It is confirmed from these figures that the reasonable results are obtained by the present measuring method except the region just behind the cylinder.

Periodically Fluctuating Velocity Vector Fields

Fig.9(a)~(h) show the periodically fluctuating velocity vector fields which are extracted by subtracting the time mean velocity vectors from the phase-averaged velocity vectors at each measuring point. The Kármán vortices rolling up behind the cylinder and moving downstream are also clearly visualized. The changing of the direction of the velocity vector just behind the cylinder, at the shoulder of the cylinder, suggests that the counterclockwise rotating vortex is shed from the lower-side of the cylinder between Phase 1 and Phase 5. Additionally, in the same way, the clockwise rotating vortex seems to shed from the upper-side of the cylinder between Phase 17 and Phase 21 that are shifted from Phase 1 and Phase 5 by half the shedding period of Karman vortex, respectively.

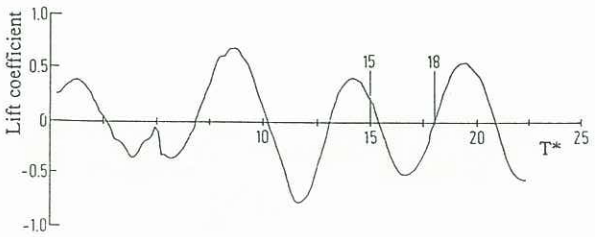

Fig.7 Time history of lift coefficient

CONCLUDING REMARKS

The phase-averaged velocity vector fields were measured by a hot-wire probe of three wires type in the near-wake flow field of the circular cylinder. The measurement was based on the *general* response equations of the hot-wires. Both flow fields of the phase-averaged and periodically fluctuating velocity vector fields were visualized by CAFV technique. The experimental results obtained in this experiment are considerably reasonable. As a result, it is concluded that the measuring method proposed here is effective and applicable to measure complex flow fields associated with periodically fluctuating phenomena.

REFERENCES

PERRY, AE, CHONG, MS and LIM, TT (1982) The vortex-shedding process behind two-dimensional bluff bodies. J Fluid Mech, 116, 77-90.

CANTWELL, B and COLES, D (1983) An experimental study of entrainment and transport in the turbulent near wake of a circular cylinder. J Fluid Mech, 136, 321-374.

TANAKA, S and MURATA, S (1985) An investigation of wake structure of a circular cylinder using a computer aided flow visualization (1st report, generation and dissipation of vorticities). Trans Japan Soc Mech Eng, 51, 2838-2845 (in Japanese).

YOSHINO, F, WAKA, R and HAYASHI, T (1989) Hot-wire direction-error response equations in two-dimensional flow. J Phys E: Sci Instrum, 22, 480-490.

INAMURO, T (1988) Numerical simulation of separated flow by discrete vortex method. J Japan Soc Fluid Mech, 7, 104-122 (in Japanese).

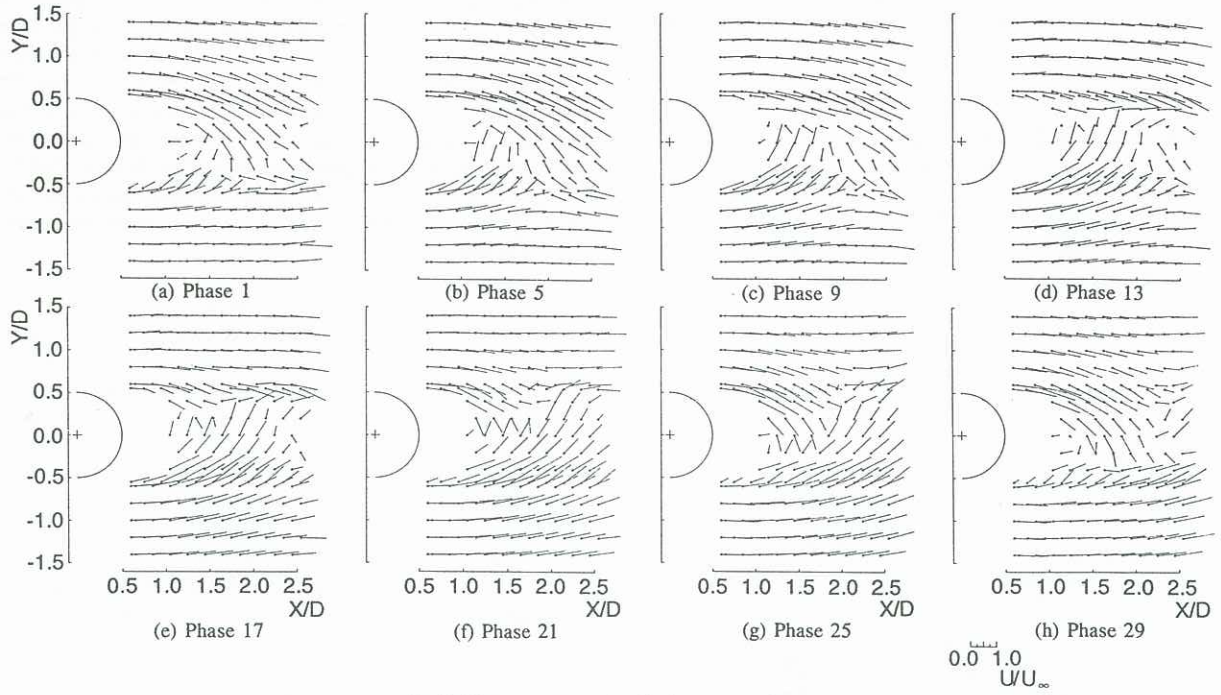

Fig.8 Phase-averaged velocity vector fields

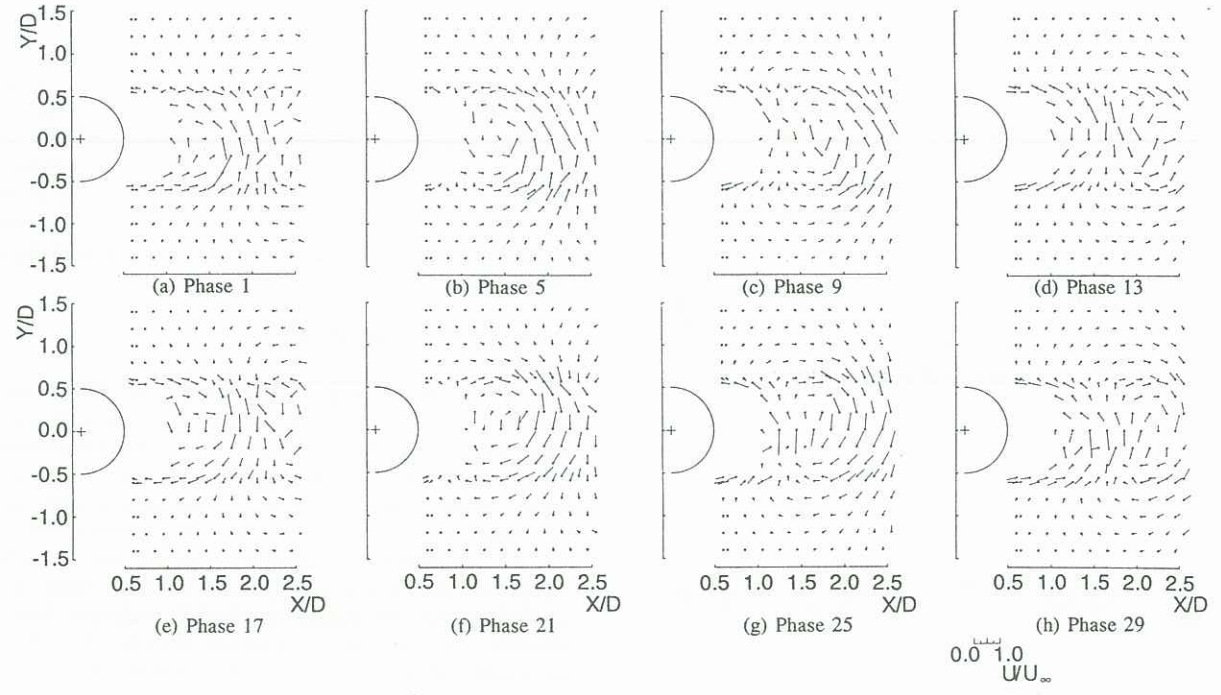

Fig.9 Periodically fluctuating velocity vector fields